

# Estimating Aggregate Cardiomyocyte Shortening Using Diffusion and Displacement Encoded MRI

Ilya A. Verzhbinsky, Luigi E. Perotti, , Kévin Moulin, Michael Loecher,  
Daniel B. Ennis

## Synopsis (100 words)

Changes in the orientation and deformation of left ventricular cardiomyocyte aggregates underlie many forms of cardiovascular disease. Despite its mechanistic significance, however, there exists no established technique to measure *in vivo* cardiomyocyte shortening ( $E_{ff}$ ). In this work, we present a pipeline to compute  $E_{ff}$  using multi-slice Displacement Encoded with Stimulated Echoes MRI and *in vivo* cardiac Diffusion Tensor Imaging data. We show that  $E_{ff}$  computed in healthy swine has decreased transmural variability compared to radial and circumferential strains. The spatial uniformity and mechanistic significance of  $E_{ff}$  make it a suitable candidate for use in the early detection of cardiac dysfunction.

## Body (750 words)

### Introduction:

Changes in the orientation and deformation of left ventricular (LV) cardiomyocyte aggregates (i.e. “myofibers”) underlie many forms of cardiovascular disease (e.g., dilated cardiomyopathy<sup>1</sup> and hypertrophic cardiomyopathy<sup>2</sup>). Global metrics of LV function, such as ejection fraction, are mainstays in the diagnosis of cardiovascular disease, but provide no tissue-level insights into the mechanisms of LV dysfunction. At the tissue level, cardiomyocyte aggregate shortening is the functional basis for gross heart contraction. Despite its mechanistic significance, however, there exists no established technique to measure *in vivo* cardiomyocyte performance.

Regional myocardial motion can be characterized at high spatial resolution using Displacement ENcoded with Stimulated Echoes (DENSE) MRI, a technique that encodes tissue displacement into the phase of the complex MRI signal. DENSE motion data is typically characterized along an anatomically defined coordinate system, e.g., circumferential ( $E_{cc}$ ), radial ( $E_{rr}$ ), and longitudinal ( $E_{ll}$ ) strains<sup>3</sup>. However, recent advances<sup>4,5</sup> in cardiac Diffusion Tensor Imaging (cDTI) allow imaging of *in vivo* cardiomyocyte aggregate orientations, which enables estimating “myofiber” strain ( $E_{ff}$ ).

Previous work in our group has measured *in vivo*  $E_{ff}$  using single-slice DENSE and cDTI data<sup>6,7</sup>. However, using single-slice DENSE displacement data requires the incorporation of mathematical assumptions to compute  $E_{ff}$ , which may confound *in vivo* estimates. The objectives of this work were: 1) to directly compute *in vivo*  $E_{ff}$  without mathematical assumptions using multi-slice DENSE MRI and cDTI data; and 2) to compare the spatial uniformity of  $E_{ff}$  with anatomically defined metrics of cardiac strain.

## Methods:

cDTI Acquisition – CINE DENSE MRI and cDTI data were acquired in healthy swine (N=8) at 3T (Prisma, Siemens). LV microstructure was measured with *in vivo* cDTI at a single mid-ventricular slice location (Fig. 1A) at mid-systole using a CODE motion compensated gradient waveform<sup>4</sup>: 2x2x5mm, TE/TR=74/4000ms, b-value=0,350s/mm<sup>2</sup>, N<sub>avg</sub>=30, N<sub>dir</sub>=12. At each cDTI voxel, the preferential cardiomyocyte aggregate orientation was defined as the primary eigenvector of the reconstructed diffusion tensors (Fig. 1D-E).

DENSE Acquisition – LV displacements were captured at two short-axis locations spaced 4mm above and below the cDTI data<sup>9</sup> (Fig. 1A) using a DENSE MRI sequence: 15ms view-shared temporal resolution (29-39 cardiac phases depending on R–R interval), 2.5x2.5x8mm voxel size, balanced 4-point phase encoding in x,y,z, TE/TR=1.04/15ms, k<sub>e</sub>=0.08cycles/mm, N<sub>avg</sub>=3, spiral interleaves=10. Using an open-source MatLab tool<sup>8</sup>, the measured x, y and z phase data were spatiotemporally unwrapped to yield voxel-wise, time-resolved Lagrangian LV displacements (Fig. 1B-C).

DENSE + cDTI Analysis – The DENSE displacement field surrounding the cDTI data was interpolated and differentiated to the location of cDTI LV voxels using the mesh-free scheme outlined in Arroyo and Ortiz<sup>10</sup>. The deformation gradient tensor (**F**) for all imaged cardiac phases was computed at the center of each voxel in the cDTI LV image. The determinant of **F** was used to evaluate tissue incompressibility. Strains at each point were computed as:

$$E_{vv} = \frac{1}{2} (\mathbf{v} \cdot \mathbf{Cv} - 1),$$

where  $\mathbf{C}=\mathbf{F}^T\mathbf{F}$  and **v** represents the direction along which the strain is computed, i.e., circumferential (E<sub>cc</sub>), radial (E<sub>rr</sub>), longitudinal (E<sub>ll</sub>), and cardiomyocyte (E<sub>ff</sub>) (Fig. 1F).

## Results:

Fig. 2 shows E<sub>ff</sub> and cardiomyocyte aggregate orientation results for a representative subject from beginning to end systole. Median (95% range) tissue incompressibility measured from the DENSE displacement field at peak systole was 4.1% (1.4%, 7.5%) across all subjects (Fig. 3).

E<sub>cc</sub>, E<sub>rr</sub>, E<sub>ll</sub> and E<sub>ff</sub> results through time are shown in Fig. 4. Median (95% range) strains across all subjects were: E<sub>ff</sub> = -0.18 (-0.23, -0.13), E<sub>cc</sub> = -0.18 (-0.24, -0.13), E<sub>rr</sub> = 0.22 (0.16, 0.30), and E<sub>ll</sub> = -0.13 (-0.19, -0.08).

For all subjects, mean±SD transmural gradient from endocardium to epicardium at peak systole were 0.03±0.04 for E<sub>ff</sub>, 0.14±0.06 for E<sub>cc</sub> (Fig. 5), -0.13±0.18 for E<sub>rr</sub>, and 0.01±0.05 for E<sub>ll</sub>.

## Discussion:

This study represents the first investigation of *in vivo* cardiomyocyte shortening using multi-slice DENSE MRI, which eliminates the need for incorporating mathematical assumptions in the computation of **F**.

Peak systolic tissue incompressibility for all subjects showed good agreement with reported myocardium quasi-incompressibility<sup>11</sup>, suggesting that the displacement field captured using DENSE MRI had low volumetric distortion.

$E_{ff}$  showed significantly reduced through-wall variability when compared to  $E_{cc}$  and  $E_{rr}$  ( $p < 0.001$ ).  $E_{ff}$  showed similarly low transmural variability to  $E_{ll}$ . The definition of the longitudinal axis, however, is somewhat arbitrary as it depends heavily on the orientation and position of the imaging location, whereas the “fiber” direction is directly measured from the tissue microstructure.

### **Conclusion:**

In this work, we demonstrate that  $E_{ff}$  can be estimated entirely from *in vivo* MRI data and provides a spatially uniform, microstructurally-anchored characterization of LV function. The spatial uniformity and mechanistic significance of  $E_{ff}$  makes it a suitable candidate for use in the early detection of cardiac dysfunction.

### **References (750 words)**

- 1 - Luk A, Ahn E, Soor GS, Butany J. Dilated cardiomyopathy: a review. *Journal of clinical pathology*. 2009 Mar 1;62(3):219-25.
- 2 - Olivetto I, Cecchi F, Poggesi C, Yacoub MH. Developmental origins of hypertrophic cardiomyopathy phenotypes: a unifying hypothesis. *Nature reviews cardiology*. 2009 Apr;6(4):317.
- 3 - Zhong X, Spottiswoode BS, Meyer CH, Kramer CM, Epstein FH. Imaging three-dimensional myocardial mechanics using navigator-gated volumetric spiral cine DENSE MRI. *Magnetic resonance in medicine*. 2010 Oct;64(4):1089-97.
- 4 - Aliotta E, Wu HH, Ennis DB. Convex optimized diffusion encoding (CODE) gradient waveforms for minimum echo time and bulk motion-compensated diffusion-weighted MRI. *Magnetic resonance in medicine*. 2017 Feb;77(2):717-29.
- 5 - Stoeck CT, Von Deuster C, Genet M, Atkinson D, Kozerke S. Second order motion compensated spin-echo diffusion tensor imaging of the human heart. *Journal of Cardiovascular Magnetic Resonance*. 2015 Dec;17(1):P81.
- 6 - Perotti LE, Magrath P, Verzhbinsky IA, Aliotta E, Moulin K, Ennis DB. Microstructurally Anchored Cardiac Kinematics by Combining In Vivo DENSE MRI and cDTI. In *International Conference on Functional Imaging and Modeling of the Heart 2017* Jun 11 (pp. 381-391). Springer, Cham.
- 7 - Magrath P, Perotti LE, Aliotta E, Verzhbinsky IA, Moulin K, Ennis DB. In Vivo Assessment of Cardiomyocyte Performance Using Combined Cardiac DENSE and cDTI. *ISMRM 2018*.
- 8 - Spottiswoode BS, Zhong X, Hess AT, Kramer CM, Meintjes EM, Mayosi BM, Epstein FH. Tracking myocardial motion from cine DENSE images using spatiotemporal phase unwrapping and temporal fitting. *IEEE transactions on medical imaging*. 2007 Jan;26(1):15-30.  
Code available at: <https://github.com/denseanalysis/denseanalysis>

9 - Verzhbinsky IA, Magrath P, Aliotta E, Ennis DB, Perotti LE. Time resolved displacement-based registration of in vivo cDTI cardiomyocyte orientations. In Biomedical Imaging (ISBI 2018), 2018 IEEE 15th International Symposium on 2018 Apr 4 (pp. 474-478). IEEE.

10 - Arroyo M, Ortiz M. Local maximum-entropy approximation schemes: a seamless bridge between finite elements and meshfree methods. International journal for numerical methods in engineering. 2006 Mar 26;65(13):2167-202.

11 - Yin FC, Chan CC, Judd RM. Compressibility of perfused passive myocardium. American Journal of Physiology-Heart and Circulatory Physiology. 1996 Nov 1;271(5):H1864-70.

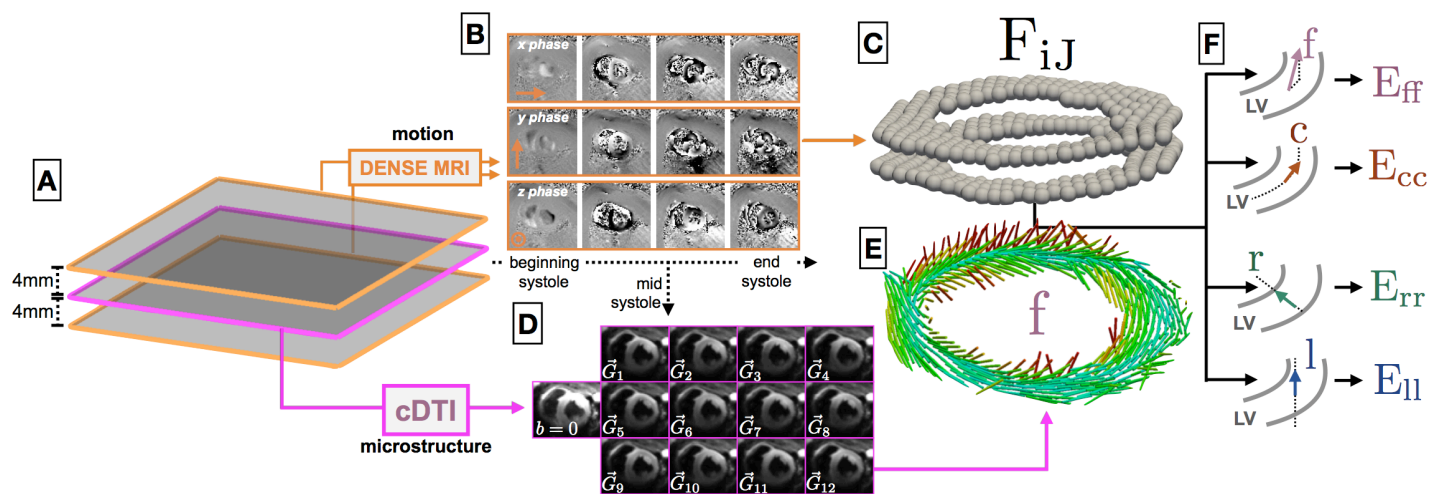


**Fig 1.** Experimental Pipeline. A) DENSE MRI was acquired 4mm above and below the cDTI location. B) Example of acquired phase data in x, y, and z throughout systole. C) Processed 3D Lagrangian displacements used to compute the deformation gradient tensor at the cDTI location. D) Example of mid-systolic diffusion weighted images ( $G_1 - G_{12}$ ) acquired in one subject using *in vivo* cDTI. E) Preferential cardiomyocyte orientations for each voxel of the cDTI data. F) Schematic demonstrating how the fiber, circumferential, radial, and longitudinal directions are computed. The two gray curves represent the epi- and endocardial contours of the LV.

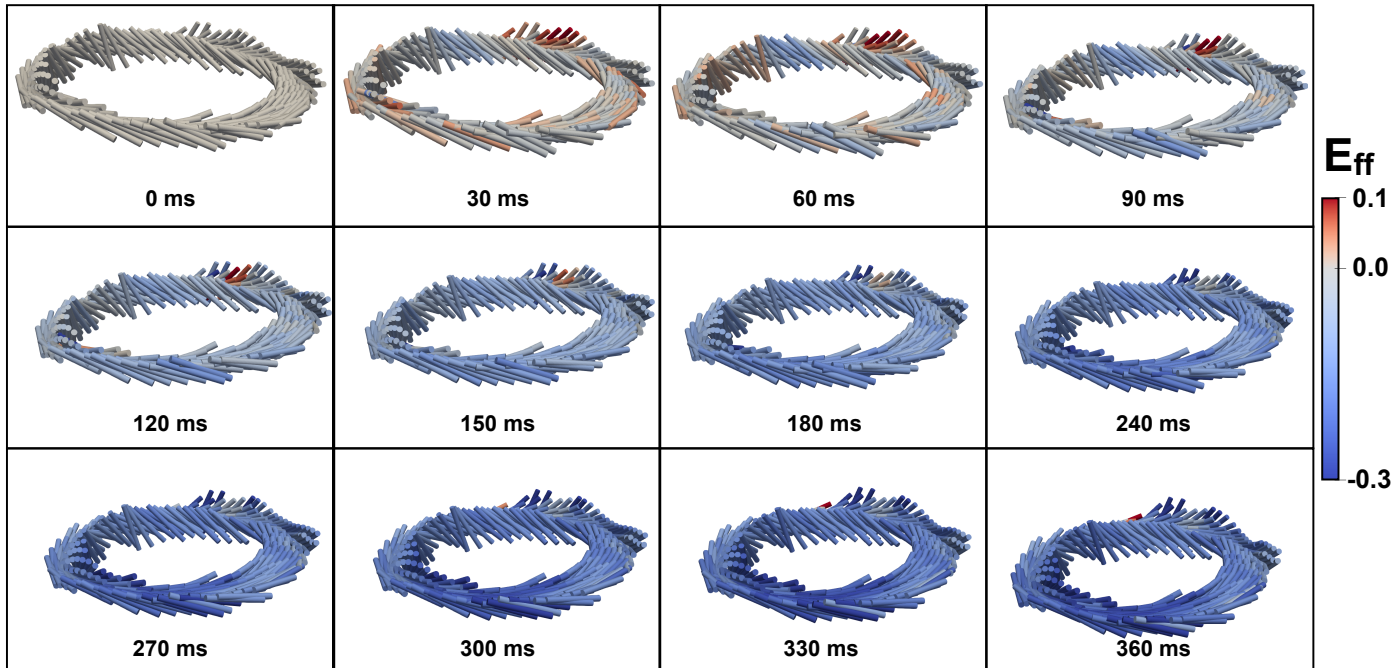


**Fig 2.** Time resolved myofiber orientations and shortening values for one subject. All times are reported with respect to the beginning of systole.

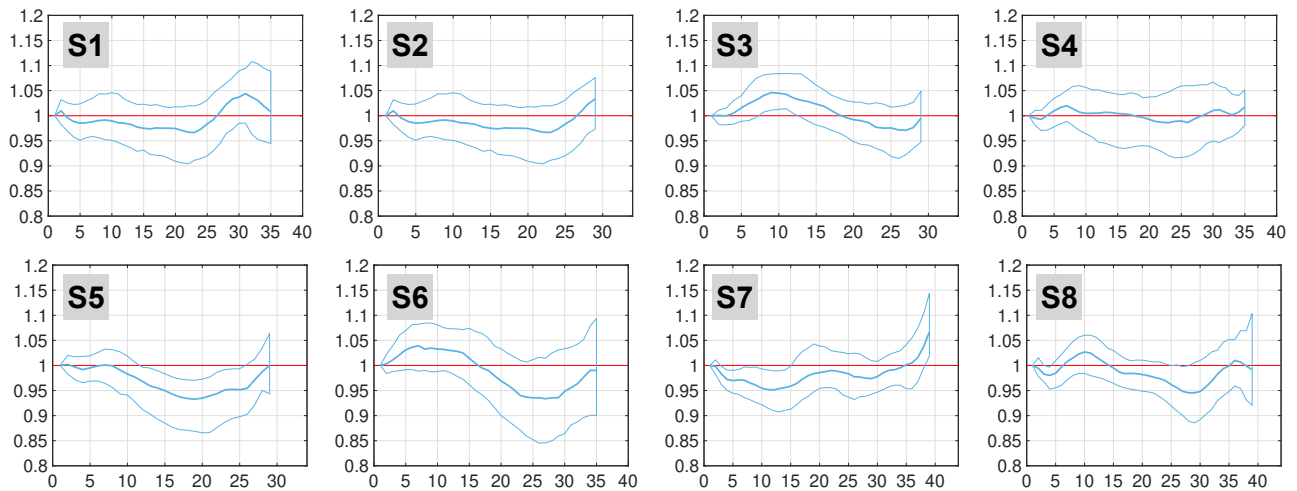


**Fig 3.** Results for tissue incompressibility through time across all subjects (S1-S8) as computed via the Jacobian of the deformation gradient tensor. Solid blue line represents the median at each cardiac phase, and thin blue line represents the 25<sup>th</sup> and 75<sup>th</sup> quartiles. A Jacobian of 1 (horizontal red line) denotes perfectly incompressible myocardium. Previous studies of myocardial compressibility report values between 2-4% (Jacobian of 0.96-0.98). Lower values at peak systole are consistent with compression of the vascular compartment during this phase.

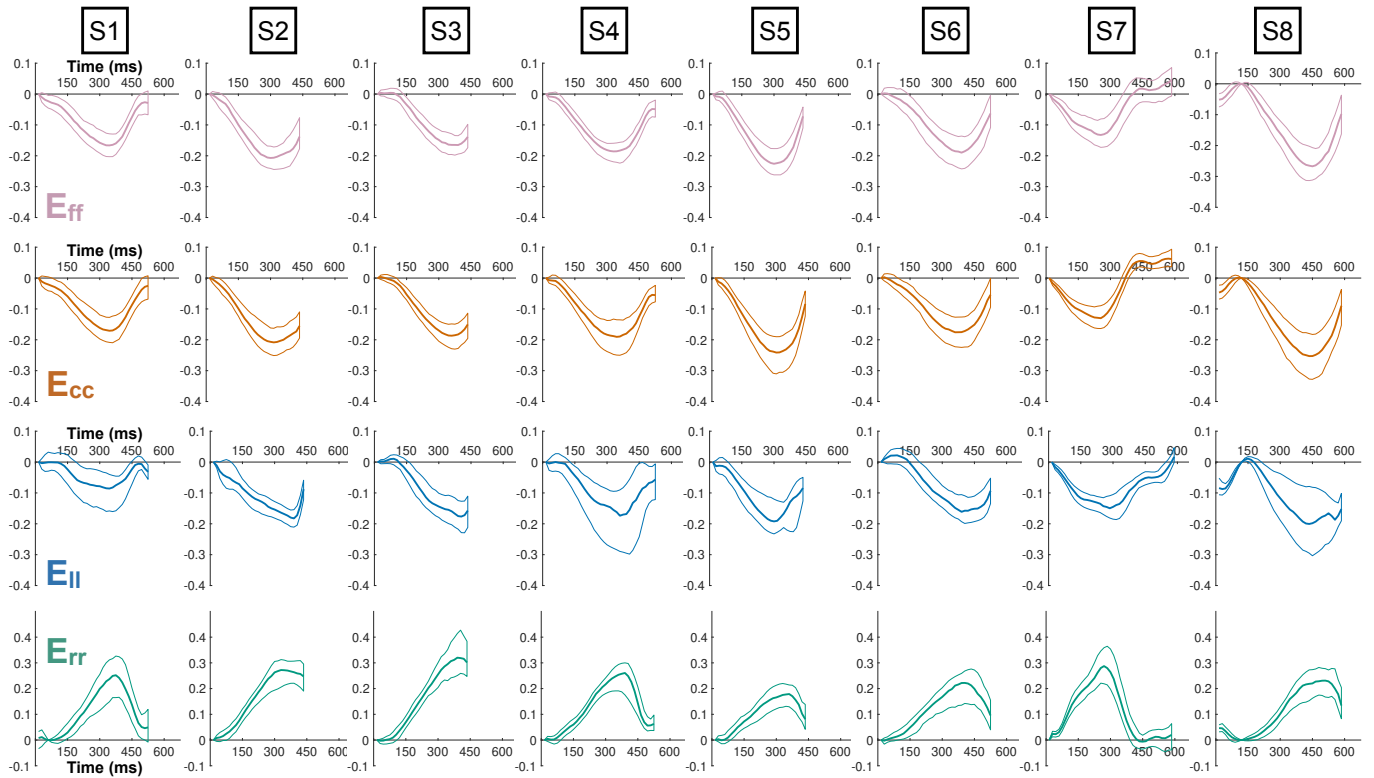


**Fig 4.** E<sub>ff</sub>, E<sub>cc</sub>, E<sub>ll</sub> and E<sub>rr</sub> results through time across all imaged subjects (S1-S8). Solid lines represent the median at each cardiac phase, while thin lines represent the 25<sup>th</sup> and 75<sup>th</sup> quartiles. The reference state for all strains (i.e., E<sub>w</sub> = 0) was defined as the beginning of systole. Note the decreased spread of E<sub>ff</sub> at peak systole.

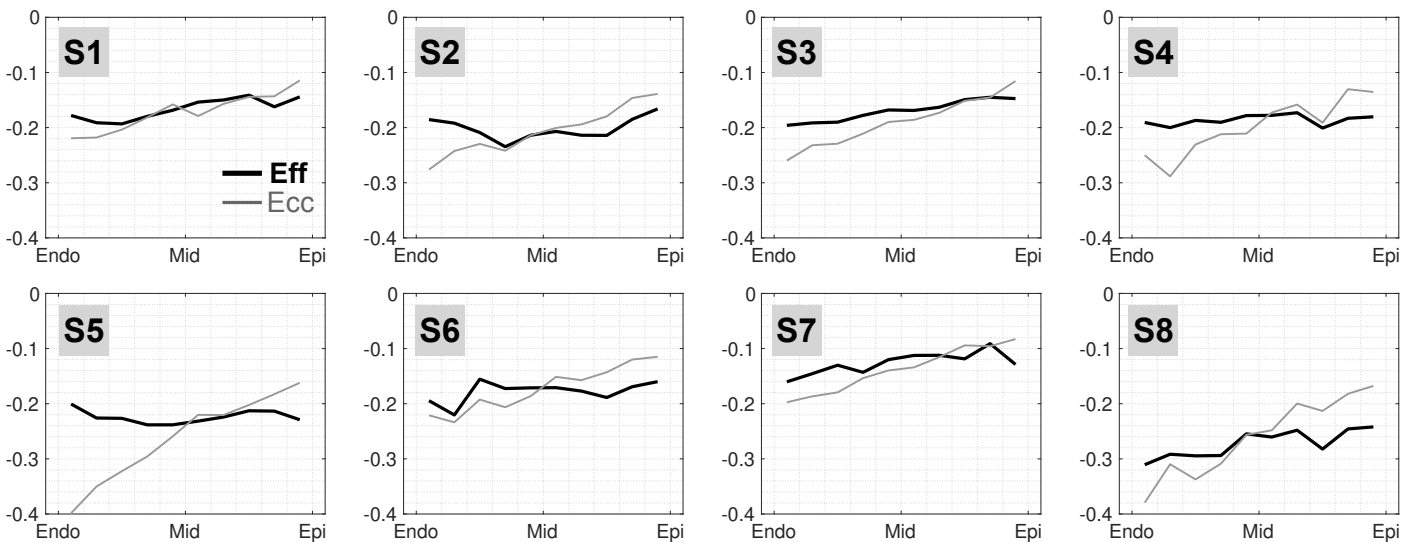


**Fig 5.** Transmural trends for E<sub>ff</sub> (black) and E<sub>cc</sub> (grey) values at peak systole. All strain data was placed into 10 transmural bins, and the medians at each bin are shown. Note the decreased spatial variability of E<sub>ff</sub> as denoted by a more horizontal transmural trend.